Robustness Analysis of a Self-Sensing AMB by Means of μ-Analysis

P.A. van Vuuren[1,a], G. van Schoor[1,b], W.C. Venter[1,c]
[1]School of Electrical, Electronic and Computer Engineering, North-West University, Potchefstroom, 2520, South-Africa
[a]Pieter.VanVuuren@nwu.ac.za, [b]George.vanSchoor@nwu.ac.za, [c]Willie.Venter@nwu.ac.za

Abstract: The stability margin of a two degree-of-freedom self-sensing AMB is estimated by means of μ-analysis. The specific self-sensing algorithm implemented in this study is the direct current measurement (DCM) method. Detailed black-box models are developed for the main subsystems in the AMB by means of discrete-time system identification. Suitable excitation signals are generated for system identification in cognisance of frequency induced nonlinear behaviour of the AMB. Novel graphs that characterize an AMB's behaviour for input signals of different amplitudes and frequency content are quite useful in this regard. In order to obtain models for dynamic uncertainty in the various subsystems (namely the power amplifier, self-sensing module and AMB plant), the identified models are combined to form a closed-loop LTI model for the self-sensing AMB. The response of this closed-loop model is compared to the original AMB's response and models for the dynamic uncertainty are empirically deduced. Finally, the system's stability margin for the modelled uncertainty is estimated by means of μ-analysis. The resultant μ-analyses show that self-sensing AMBs are rather sensitive for variations in the controller and the self-sensing module.

Keywords: Robustness Analysis, μ-Analysis, System Identification, Self-Sensing AMBs

Introduction

The de facto standard for robustness estimation in the AMB literature is the sensitivity function ([1], [2], [3] and [4]). However, in [5] it is shown that the peak value of the sensitivity function only gives a necessary (but not sufficient) condition for robust stability.

Alternative MIMO robustness estimation techniques that have been applied to AMBs include the generalized Nyquist criterion [6], Kharitonov's stability theorem [6] and the ν-gap metric [7]. Of the available LTI MIMO robustness estimation techniques, μ-analysis promises to deliver the least conservative estimates of the stability margin of an AMB system.

One of the lessons from [8], [9] and [10] is that accurate robustness analysis requires that each of the constituent parts of a self-sensing AMB system be modelled accurately. A fundamental prerequisite for μ-analysis is that the system under scrutiny be modelled with an analytical LTI model. Fortunately, it is possible to closely approximate the oscillatory behaviour of switching power amplifiers by means of LTI black-box models obtained via system identification (if the order is chosen sufficiently high). Another advantage of system identification is that it doesn't have any trouble in modelling cross-coupling occurring in a system. This is a huge benefit since electromagnetic cross-coupling also has a large effect on self-sensing implemented on heteropolar AMBs ([11] and [3]).

Accurate μ-analysis requires accurate models of the nominal system as well as the uncertainty to which the model is subjected [12]. For this reason system identification is also applied to obtain accurate models for the dynamic uncertainty in the self-sensing AMB system, but more of this later on in the paper.

The rest of this paper is concerned with quick summaries of DCM self-sensing and μ-analysis. This is followed by highlights of the procedure for obtaining accurate nominal models for a self-sensing AMB by means of system identification. Finally, the results that were obtained are discussed.

DCM self-sensing

This paper's results are based on simulation studies performed with a reasonably accurate simulation model of a two degree-of-freedom (2-DOF) DCM (direct current measurement method) self-sensing AMB. More details on DCM self-sensing can be found in [13]. The accuracy of this simulation model has been established in [3]. The above mentioned simulation model consists of a PID controller, four power amplifiers, a magnetic circuit model, point mass, an ideal position sensor (for the x-axis position) and the DCM self-sensing algorithm (for the y-axis position). Two identical PID controllers (each responsible for movement along one axis of freedom) comprise the controller, while each of the four stator electromagnets is powered by its own two-state switching power amplifier. The flux distribution in the AMB magnetic circuit is modelled by means of a reluctance network model [14]. The response of the reluctance network model is enriched with two additional models: one responsible for predicting eddy currents and the other for modelling magnetic hysteresis and saturation. More details on the specific simulated AMB can be found in [15].

Summary of μ-analysis

Robust control theory is built on the notion of norm-bounded uncertainty [16]. This is a frequency domain concept where the uncertainty surrounding a particular model can be expressed by means of bounds on the norm of the model's transfer function. The traditional system blockdiagram can be rearranged to obtain the generalized form of Figure 1 [12].

In this block-diagram the controller is represented by **K**, while the nominal model of the rest of the AMB system is collected in **P** (also known as the generalized plant). $\boldsymbol{\Delta}$ is a block-diagonal matrix that consists of normbounded general uncertainties (scalars or LTI transfer functions conforming to respectively $|\Delta_m| \le 1$ and $\|\Delta_n(j\omega)\|_\infty \le 1 \; \forall \omega$ [1]). The uncertainty matrix, $\boldsymbol{\Delta}$, therefore represents general uncertainties that can impact on the parameters or dynamics of the nominal generalized plant.

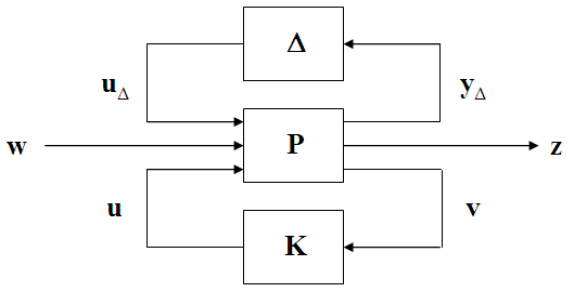

Figure 1: Generalized block diagram

The degree to which the general uncertainties in $\boldsymbol{\Delta}$ actually influence the self-sensing AMB are determined by weights (whether scalar weights or weight transfer functions). These weights are incorporated into the generalized plant **P**.

[1] Where the subscripts *m* and *n* refer to the corresponding elements in the block-diagonal matrix.

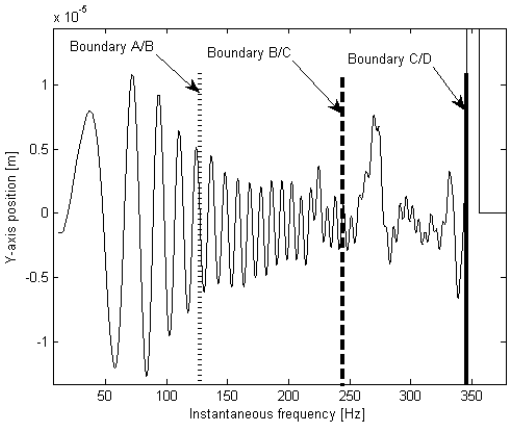

(a) Response of a nonlinear 2-DOF AMB to a frequency sweep

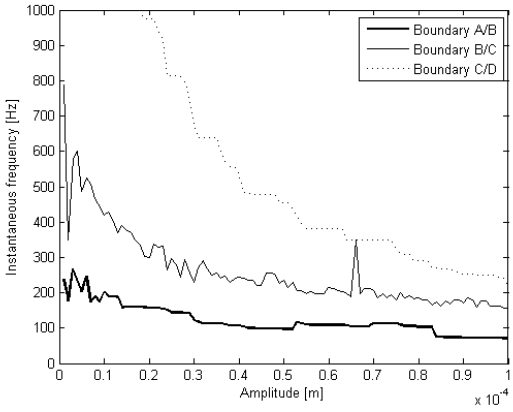

(b) Frequency-amplitude graph

Figure 2: Frequency induced nonlinearity

For the purpose of μ-analysis, the controller **K** can be combined with the generalized plant **P** by means of a lower linear fractional transformation ([12]) to obtain Eq. 1.

$$\begin{bmatrix} y_\Delta \\ z \end{bmatrix} = N \begin{bmatrix} u_\Delta \\ w \end{bmatrix} = \begin{bmatrix} N_{11} & N_{12} \\ N_{21} & N_{22} \end{bmatrix} \begin{bmatrix} u_\Delta \\ w \end{bmatrix} \tag{1}$$

The last step of μ-analysis is then to isolate the N_{11} component and to determine its structured singular value (μ). If the peak value of $\mu_\Delta(j\omega)$[2] is less than one for all frequencies, then the difference between one and the aforementioned peak value reflects the stability margin of the system.

Modelling the nominal system via system identification

Accurate robustness estimates can only be obtained via μ-analysis if the nominal system is accurately modelled by an LTI model. AMBs are however inherently nonlinear and time variant. Through the use of differential driving mode ([17]) the behaviour of the AMB rotor as a function of its position and the coil currents can be linearised over the greatest part of its operating range [15].

The magnetic force exerted by an electromagnet is however not only a nonlinear function of position and current *but also* of the frequency content of the position signal of the AMB rotor ([18] and [19]). Figure 2(a) reveals the specific nonlinear behaviour induced by the frequency of the shaft position. This figure shows the simulated response of a 2-DOF AMB (with ideal position sensors) for a reference position signal that consisted of a sine-wave frequency sweep at a constant amplitude. The AMB's behaviour may be classified into different regions of operation, namely: regions A (linear), B (affine), C (nonlinear oscillatory behaviour) and D (delevitation).

Accurate system identification depends on the quality of the excitation signal. An excitation signal that gives rise to maximally informative input and output data is known as a *persistently exciting* signal [20]. Due to the existence of frequency induced nonlinearities in AMBs it is vital to ensure that nonlinear behaviour isn't induced in the AMB by the very signal with

[2] The structured singular value is also a function of frequency.

which it is interrogated. By measuring the response of an AMB to numerous frequency sweeps (of various combinations of the amplitude and maximum frequencies) and automatically detecting the boundaries between the different regions of AMB behaviour ([15]), it is possible to predict the degree to which an AMB will behave in a nonlinear fashion for various input signals. An example of such a frequency-amplitude graph (obtained for a similar AMB equipped with ideal position sensors) is shown in Figure 2(b).

To ensure LTI operation of the AMB, the frequency-amplitude graph advises that the spectral composition of the excitation signals should be biased toward low-frequency components rather than high frequency components. What is required is an excitation signal whose spectral content can be constrained to be within a narrow band. Examples of such signals are random phase multi-sine signals and rectangular waves.

AMBs are inherently unstable, which implies that system identification can only be performed while the AMB is in closed-loop operation. This is known as direct closed-loop identification [20]. In order to minimize distortion, the excitation signal must be injected as closely possible to the specific module that is to be modelled [15]. In this study excitation signals were therefore injected between the PID controller and the power amplifiers.

The weakest link in an LTI model for a self-sensing AMB is the power amplifier model. This is because a switching power amplifier's response is not only a function of the controller output, but also of the actual position of the mass within the airgap. The LTI model of the power amplifiers should therefore be an explicit function of all variables that have an effect on the real coil currents, namely the outputs of the controller as well as the position of the rotor within the airgap. The identified power amplifier model is therefore a four-input, four-output discrete-time state-space model obtained via subspace parameter estimation [20]. Finally, the rest of the AMB plant (the stator, coils and point-mass) is modelled by a four-input, two-output model. (In contrast, DCM self-sensing is modelled by a SISO model, since the y-axis position can be estimated solely from the maximum values of the current ripple on a single AMB coil current signal.)

The *de facto* procedure in μ-analysis is to convert the discrete-time model to an equivalent continuous-time model prior to calculating the values of μ. Since the latter conversion tends to amplify any errors made during discrete-time parameter estimation by a factor approximately equal to the sampling frequency [15] (which is 83.3 kHz), it is vitally important to obtain very accurate discrete-time models for the various AMB sub-components.

Uncertainty modelling

The dominant contributor towards dynamic uncertainty in self-sensing AMBs is the occurrence of nonlinear behaviour that can't be modelled in the LTI paradigm. The process of modelling this mismatch entails two steps ([21], [22]). Firstly, the "difference" between the model and real system is measured empirically. Secondly, the measured differences are summarized by means of a simplified transfer function.

Assuming that the dominant cause of dynamic uncertainty in the AMB is due to unmodelled high-frequency dynamics, the mismatch between the real system $G(s)$ and its nominal model $\overline{G}(s)$ can be modelled by means of additive uncertainty as follows [12]:

$G(s) = \overline{G}(s) + W(s)\Delta(s)$, where $W(s)$ represents the uncertainty weight transfer function.

With the general norm-bounded uncertainty $\Delta(s)$ constrained as follows: $\left\|\Delta(j\omega)\right\|_\infty \le 1 \,\forall\, \omega$, the empirical transfer function estimate (ETFE) of the uncertainty weight for additive uncertainty can be calculated from the following inequality: $\left|(W(s)\right| \ge \left|\frac{Y(s)}{X(s)} - \frac{\overline{Y}(s)}{\overline{X}(s)}\right|$, where the spectra of the input and output signals of the real system are represented by $X(s)$ and $Y(s)$ respectively. Similarly, the input and output spectra of the nominal model are given by $\overline{X}(s)$ and $\overline{Y}(s)$ respectively.

The second step of the uncertainty modelling process entails summarizing the ETFEs by means of analytical models. The de facto practice in the literature is to fit a smooth function which acts as an upper bound to the measured frequency response [12], [22] and [21]. Various means exist to accomplish this purpose. One potential solution entails finding a number of peaks in the ETFE and connecting them with low order curves. Finally, zeros and poles are iteratively added in accordance with the well-known first order asymptotic approximations for Bode plots until the deviation between the observed ETFE and the fitted function is below a pre-defined threshold. As an example, Figure 3 shows the results of the above mentioned algorithm when applied to one of the SISO uncertainty weight ETFEs in the AMB plant uncertainty model.

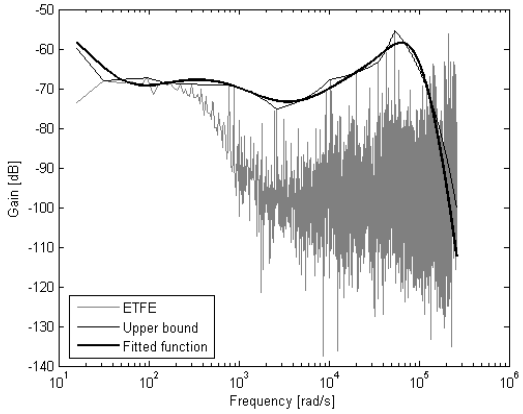

Figure 3: Fitting a transfer function to an ETFE

Results

Validation of the nominal model. The final nominal closed-loop LTI model of the 2-DOF self-sensing AMB of this study consisted of the following discrete-time state-space models ([15]): a 9th order AMB plant model (4 inputs, 2 outputs); a 7th order power amplifier model (4 inputs, 4 outputs) and a 3rd order SISO model for DCM self-sensing. Figure 4(a) shows the responses of both the original nonlinear simulation as well as the identified closed-loop LTI model on the same data used for system identification. Clearly the identified self-sensing model is at fault, drastically reducing the bandwidth and fidelity of the total closed-loop system. Poor performance of LTI models for nonlinear systems containing "hard" nonlinearities such as the maximum-operator used in DCM self-sensing ([3]) is however to be expected.

Robustness analysis for parametric uncertainty in the controller. The 2-DOF selfsensing AMB is controlled by means of two identical, decoupled PID controllers. The effect of variability in the individual PD controller coefficients of a comparable 2-DOF equipped with ideal position sensors is summarized in Table 1. Clearly, μ-analysis predicts that the AMB will remain robustly stable for individual coefficient perturbations in excess of 80 % from the nominal value. These predictions are however contradicted by Monte Carlo analyses performed on both the identified nominal LTI AMB model and the original nonlinear simulation model. These Monte Carlo analyses estimated the probability of instability for the

stated allowable coefficient variability. It is clear from the Monte Carlo analyses that LTI modelling gives an optimistic assessment of the system's true stability margin. This error is further compounded during μ-analysis.

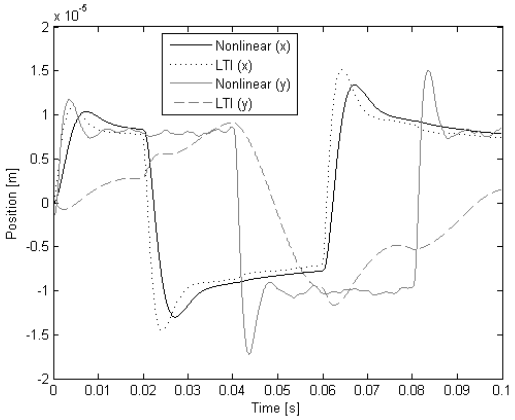

(a) Performance of the nominal closed-loop AMB model

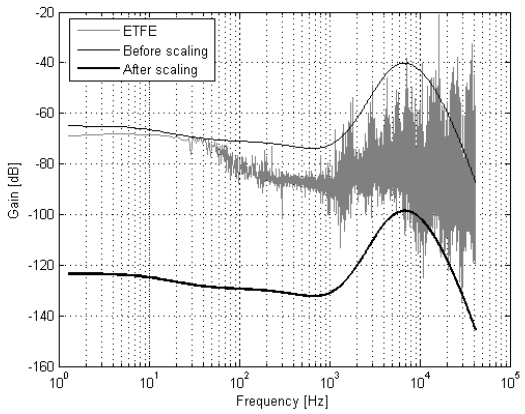

(b) Uncertainty model for the self-sensing module

Figure 4: DCM selfsensing

Table 1: Robustness analysis for controller parametric uncertainty in the sensed AMB

Deviation in K_P [%]	Deviation in K_D [%]	Peak value of μ	Probability of instability (LTI) [%]	Probability of instability (nonlinear) [%]
80	0.1	0.34	12	37
0.1	80	0.56	11	33

The effect of parametric uncertainty in the PID controller coefficients of the self-sensing AMB is summarized in table 2. Once again, μ-analysis is shown to be over-optimistic in its robustness estimations. The results in Tables 1 and 2 however also show that DCM self-sensing is more sensitive to variations in the controller parameters than normal AMBs.

Table 2: Robustness analysis for controller parametric uncertainty in the selfsensing AMB

Deviation in K_P [%]	Deviation in K_D [%]	Deviation in K_I [%]	Peak value of μ	Probability of instability (LTI) [%]	Probability of instability (nonlinear) [%]
19	0.1	0.1	0.98	100	0
0.1	80	0.1	0.93	85	51
0.1	0.1	10	0.94	100	40

Robustness analysis for dynamic uncertainty in DCM self-sensing. The effect of dynamic uncertainty occuring in the self-sensing module on the closed-loop system's stability margin can be assessed as follows. First of all a random-phase multi-sine signal (with an amplitude of 100 μm and frequency content stretching from 5 Hz to 26 Hz) is applied to the system input. From this excitation signal the additive uncertainty weight in Figure 4(b) is estimated. According to the modelled uncertainty, the nominal LTI self-sensing model's primary shortcoming is its high-frequency behaviour.

Unfortunately the conservatism of μ-analysis requires that the fitted uncertainty weight function be scaled down by a factor of 0.0012. The resultant μ-plot is shown in Figure 5(a).

Even though a 2 Hz component isn't visible in the uncertainty weight in Figure 4(b), this component is the dominant factor in the μ-plot. From the μ-plot we can deduce that the closed-loop system's stability margin for dynamic uncertainty in the self-sensing module is dominated by an extreme sensitivity for the critical frequency of the AMB plant. The robustness of a selfsensing AMB for general dynamic uncertainty can therefore be improved by better control at this frequency.

The LTI uncertainty model is however totally unsuited to analyse the effect of nonlinear phenomena on the stability margin of the self-sensing AMB. This is once again proved by applying a 99 μm amplitude frequency sweep signal stretching from 11 Hz to 50 Hz at the system input. Neither the nominal LTI closed-loop model, nor the augmented model (consisting of the nominal model and uncertainty weights) could correctly predict delevitation (as can be seen in Figure 5(b)).

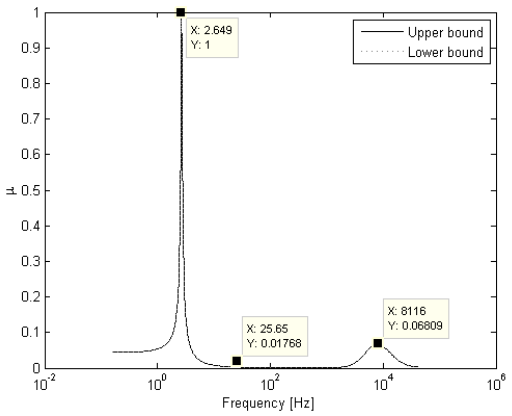

(a) μ-plot for dynamic uncertainty in the self-sensing module

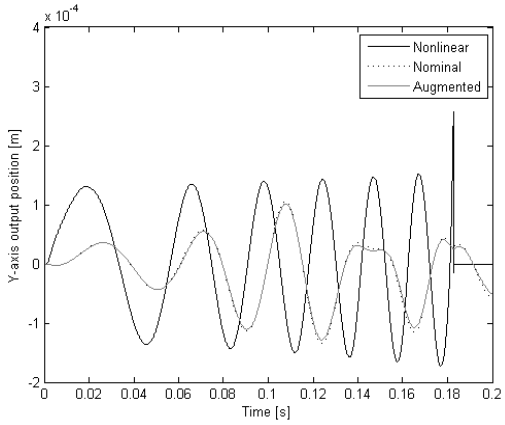

(b) Responses to a frequency sweep

Figure 5: Results

Conclusions

The fundamental issue at stake is the validity of modelling a mismatch between a nonlinear system and an LTI nominal model by means of another LTI model (the uncertainty model). An example of this problem is the inability of μ-analysis to predict delevitation due to frequency induced nonlinearities in the AMB (e.g. in Figure 5(b)). Since the augmented model couldn't correctly model region B and C behaviour, the prime cause of the problem lies at the door of the LTI uncertainty weight.

Nonetheless, the μ-plots obtained for dynamic uncertainty in the AMB are quite useful to identify specific frequencies where the system is especially fragile.

Self-sensing AMBs are nonlinear multivariable systems. This paper has shown that a linearization approach to the robustness analysis of this system isn't sufficient. Accurate robustness analysis requires accurate models of the nominal system and the expected uncertainty. Further work should therefore be done on the development of an analytical nonlinear model for a self-sensing AMB.

References

[1] "1st ISO/CD 14839-3 "Mechanical vibration vibration of rotating machinery equipped with active magnetic bearings part 3: Evaluation of stability margin"," International Organization for Standardization, Committee draft standard ISO/TC 108 / SC 2, October 2003.

[2] A. Schammass, “A self-sensing active magnetic bearing: modulation approach,” Ph.D. dissertation, EPFL, Switzerland, 2003.
[3] A. Niemann, “Self-sensing algorithms for active magnetic bearings,” Ph.D. dissertation, North-West University, 2008.
[4] E. Ranft, “An improved model for self-sensing heteropolar active magnetic bearings,” Ph.D. dissertation, North-West University (Potchefstroom campus), 2007.
[5] G. Li, E. H. Maslen, and P. Allaire, “A note on ISO AMB stability margin,” in Proceedings of the 10th International Symposium on Magnetic Bearings, Martigny, Switzerland, 2006.
[6] N.-C. Tsai, C.-H. Kuo, and R.-M. Lee, “Regulation on radial position deviation for vertical amb systems,” Mechanical Systems and Signal Processing, vol. 21, pp. 2777–2793, 2007.
[7] G. Li, “Robust stabilization of rotor-active magnetic bearing systems,” Ph.D. dissertation, University of Virginia, 2007.
[8] N. Morse, R. Smith, B. Paden, and J. Antaki, “Position sensed and self-sensing magnetic bearing configurations and associated robustness limitations,” in Proceedings of the 37th IEEE conference on decision and control, December 1998, pp. 2599–2604.
[9] E. Maslen, D. Montie, and T. Iwasaki, “Robustness limitations in self-sensing magnetic bearings,” Journal of dynamic systems, measurement, and control, vol. 128, pp. 197–203, June 2006.
[10] E. Maslen, T. Iwasaki, and R. Mahmoodian, “Formal parameter estimation for self-sensing,” in Proceedings of the tenth international symposium on magnetic bearings, Martigny, Switzerland, August 21-23 2006.
[11] N. Skricka and R. Markert, “Influence of cross-axis sensitivity and coordinate coupling on selfsensing,” in Proceedings of 6th International Symposium on Magnetic Suspension Technology, Turin, Italy, October 2001, pp. 179–184.
[12] S. Skogestad and I. Postlethwaite, Multivariable feedback control: analysis and design, 2nd ed. Chichester, UK: John Wiley & Sons, 2005.
[13] A. Niemann and G. Van Schoor, “Self-sensing algorithm for active magnetic bearings; using direct current measurements,” in Proceedings of the 12th International Symposium on Magnetic Bearings. Wuhan, China: ISMB, August 2010.
[14] D. Meeker, E. Maslen, and M. Noh, “An augmented circuit model for magnetic bearings including eddy currents, fringing, and leakage,” IEEE Transactions on Magnetics, vol. 32, no. 4, pp. 3219–3227, July 1996.
[15] P. Van Vuuren, “Robustness estimation of self-sensing active magnetic bearings via system identification,” Ph.D. dissertation, North-West University, 2010.
[16] K. Zhou, J. Doyle, and K. Glover, Robust and optimal control. Upper Saddle River, NJ: Prentice Hall, 1996.
[17] G. Schweitzer, H. Bleuler, and A. Traxler, Active Magnetic Bearings: Basics, Properties and Applications of Active Magnetic Bearings. Z¨urich: Authors Reprint, 2003.
[18] U. Hegazy and Y. Amer, “A time-varying stiffness rotor-active magnetic bearings system under parametric excitation,” Proc. IMechE Part C: J. Mechanical Engineering Science, vol. 222, pp. 447–458, 2008.
[19] J. Jugo, I. Lizarraga, and I. Arredondo, “Nonlinear modelling and analysis of active magnetic bearing systems in the harmonic domain: a case study,” IET Control Theory Applications, vol. 2, no. 1, pp. 61–71, 2008.
[20] L. Ljung, System identification: theory for the user, 2nd ed. Upper Saddle River, NJ: Prentice Hall, 1999.
[21] D. Bayard, Y. Yam, and E. Mettler, “A criterion for joint optimization of identification and robust control,” IEEE Transactions on Automatic Control, vol. 37, no. 7, pp. 986–991, July 1992.
[22] B. Lu, H. Choi, G. Buckner, and K. Tammi, “Linear parameter-varying techniques for control of a magnetic bearing system,” Control Engineering Practice, vol. 16, pp. 1161–1172, 2008.